THE JOURNAL OF BIOLOGICAL CHEMISTRY
Vol. 277, No. 19, Issue of May 10, pp. 17101–17107, 2002

Printed in U.S.A.

Partially Folded Structure of Flavin Adenine Dinucleotide-depleted Ferredoxin-NADP$^+$ Reductase with Residual NADP$^+$ Binding Domain*

Received for publication, December 17, 2001, and in revised form, February 27, 2002
Published, JBC Papers in Press, February 28, 2002, DOI 10.1074/jbc.M112002200

Masahiro Maeda, Daizo Hamada‡, Masaru Hoshino, Yayoi Onda§, Toshiharu Hase, and Yuji Goto¶

From the Institute for Protein Research, Osaka University, 3-2 Yamadaoka, Suita, Osaka 565-0871, Japan

Maize ferredoxin-NADP$^+$ reductase (FNR) consists of flavin adenine dinucleotide (FAD) and NADP$^+$ binding domains with a FAD molecule bound noncovalently in the cleft between these domains. The structural changes of FNR induced by dissociation of FAD have been characterized by a combination of optical and biochemical methods. The CD spectrum of the FAD-depleted FNR (apo-FNR) suggested that removal of FAD from holo-FNR produced an intermediate conformational state with partially disrupted secondary and tertiary structures. Small angle x-ray scattering indicated that apo-FNR assumes a conformation that is less globular in comparison with holo-FNR but is not completely chain-like. Interestingly, the replacement of tyrosine 95 responsible for FAD binding with alanine resulted in a molecular form similar to apo-protein of the wild-type enzyme. Both apo- and Y95A-FNR species bound to Cibacron Blue affinity resin, indicating the presence of a native-like conformation for the NADP$^+$ binding domain. On the other hand, no evidence was found for the existence of folded conformations in the FAD binding domains of these proteins. These results suggested that FAD-depleted FNR assumes a partially folded structure with a residual NADP$^+$ binding domain but a disordered FAD binding domain.

Protein folding is one of the most important issues in structural biology and many other related fields in molecular biology and biotechnology. The characterization of an intermediate state between the native and unfolded structures is important in understanding the folding mechanism of proteins (1, 2). Although many small proteins of <100 amino acids in length show highly cooperative folding reactions from the unfolded to the native state without accumulating observable intermediates, proteins with >100 amino acid residues (3) and some smaller proteins (4, 5) show populated intermediates with partially folded structures, *e.g.* the molten globule state, in the first millisecond of folding reactions (6). For a number of proteins, partially folded intermediates with conformational properties similar to those of kinetic folding intermediates have been found under mild denaturing conditions in equilibrium (7, 8). These observations offer the opportunity to analyze the detailed conformational properties of the partially folded structures or the roles of individual subdomains.

Some large proteins can be decomposed into folding units (9, 10). The existence of several domains in such proteins is assumed to reflect both the organization of the genes and the dynamics of the folding process (11, 12). It has been proposed that domains and subdomains fold independently and subsequently merge to produce the native molecule (13). Recent studies of protein folding have focused on small proteins or domains of larger proteins. This is not only because of the simplicity of the mechanisms and reversibility of folding reactions, but also because of the probability that these reactions reflect earlier events in the folding process of larger proteins. On the other hand, the direct characterization of folding and unfolding behavior with the entire molecule is necessary for complete understanding of the folding mechanisms of larger proteins (5, 14). In the present study, we analyzed ferredoxin-NADP$^+$ reductase (FNR)[1] (EC 1.18.1.2) as an example of such a large protein.

FNR catalyzes reduction of NADP$^+$ to NADPH during photosynthesis in higher plants (15). The crystal structure of maize FNR has recently been determined by x-ray crystallography (Fig. 1) (16). The molecule was shown to be composed of well-defined FAD and NADP$^+$ binding domains. The FAD binding domain (residues 1–153) is made up of a scaffold of six antiparallel β-strands arranged in two perpendicular β-sheets, the bottom of which is capped by an α-helix and a long loop. The NADP$^+$ binding domain (residues 154–314) consists of a core of five parallel β-strands surrounded by seven α-helices. The FAD cofactor is bound to the protein through hydrogen bonds, van der Waals contacts, and π-π stacking interactions. The isoalloxazine ring system, which constitutes the reactive part of FAD, is stacked on the aromatic rings of two tyrosine residues, *i.e.* Tyr^{95} and Tyr^{314} (Fig. 1*A*).

We studied the structural properties of holo-FNR and two forms of apoenzyme, *i.e.* apo-FNR prepared by $CaCl_2$ treatment (17) and the Y95A mutant lacking FAD due to the absence of one of the stacking aromatic rings. The structure and stability of these species were analyzed by a combination of optical and physicochemical techniques including CD, small angle x-ray scattering (SAXS) and fluorescence spectrometry, pH and guanidinium hydrochloride (Gdm-HCl) denaturation, affinity chromatography, and enzymatic assay. The data suggested the formation of intermediate structures with a persistent native-

* This work was supported in part by grants-in-aid for scientific research from the Japanese Ministry of Education, Culture, Sports, Science and Technology. The costs of publication of this article were defrayed in part by the payment of page charges. This article must therefore be hereby marked "*advertisement*" in accordance with 18 U.S.C. Section 1734 solely to indicate this fact.

‡ Supported by a Japan Society for the Promotion of Science Research Fellowship for Young Scientists (PD).

§ Present address: MRC Laboratory of Molecular Biology, Hills Rd., Cambridge CB2 2QH, United Kingdom.

¶ To whom correspondence should be addressed. Tel.: 81-6-6879-8614; Fax: 81-6-6879-8616; E-mail: ygoto@protein.osaka-u.ac.jp.

[1] The abbreviations used are: FNR, ferredoxin-NADP$^+$ reductase; Gdm-HCl, guanidinium hydrochloride; SAXS, small angle X-ray scattering; FAD, flavin adenine dinucleotide.

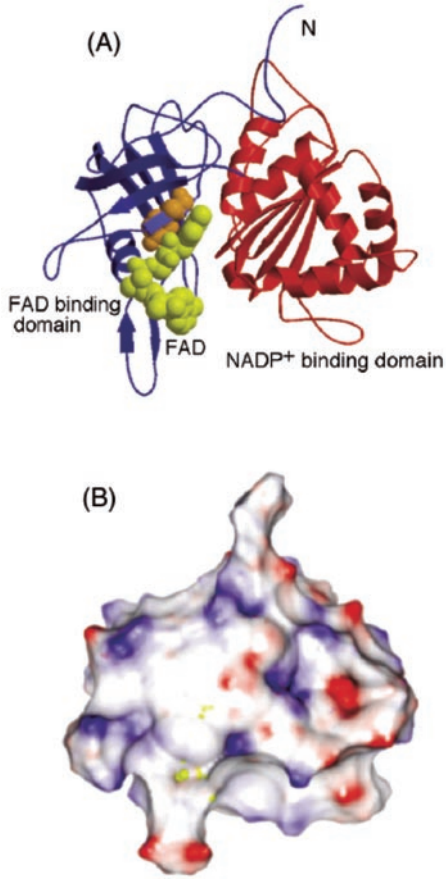

FIG. 1. **The structure of maize ferredoxin-NADP$^+$ reductase determined from x-ray crystal diffraction data.** *A*, ribbon diagram of the FAD binding domain and the NADP$^+$ binding domain, which are colored *blue* and *red,* respectively. The prosthetic group FAD (*yellow*) and Tyr^{95} (*orange*) are represented as space-filling models. *B*, the electrostatic surface potential map of holo-FNR; positively charged regions are *blue*, negatively charged regions are *red*, and FAD is *yellow*. The figure was generated with x-ray coordinates 1GAW using MOLMOL (46).

like NADP$^+$ binding domain and an unfolded FAD binding domain.

EXPERIMENTAL PROCEDURES

Protein Preparation—Recombinant maize leaf FNR (18) and ferredoxin (19) were prepared using an *Escherichia coli* expression system. Site-directed mutagenesis to obtain Y95A-FNR was carried out by PCR with a pair of primers (sense, 5′-GGCGTCGACAAGAACGGCAAGCCGCACAAGGTCAGGCTCGCTTCCATCGCCAGCAGCGCG-3′ (*underlined letters* indicate the codon for the substituted Ala); antisense, 5′-CATCGATACCCTTCTCCATGCCTTTCAACCC-3) using pYOL-FNR1 (18) as the template. PCR was carried out with a program of 25 cycles of 30 s at 98 °C and 45 s at 72 °C using KOD polymerase (Toyobo, Osaka, Japan). The resulting fragment was cut with *Sal*I and inserted into the corresponding region of pYOL-FNR1 (18). The achievement of the desired mutation and the absence of PCR errors were verified by DNA sequencing. Purification of Y95A-FNR, which was not associated with FAD, was carried out essentially according to the method used for the wild-type FNR except for Cibacron Blue affinity chromatography. Crude extract of *E. coli* cells expressing Y95A-FNR was fractionated with ammonium sulfate between 40% and 70% saturation. The resulting precipitate was dissolved in 40% ammonium sulfate and 50 mM Tris-HCl buffer (pH 7.5) and loaded onto a column of butyl-Toyopearl (Tosoh). The column was eluted with a linear gradient of 40% to 0% ammonium sulfate in 50 mM Tris-HCl buffer (pH 7.5). The fraction containing Y95A-FNR was further purified on a column of HiTrap Blue (Amersham Biosciences), which was equilibrated with 50 mM Tris-HCl buffer (pH 7.5), by developing with a linear gradient of 0–1 M NaCl in the same buffer. The purity of the enzyme was confirmed by SDS-PAGE. Sedimentation velocity ultracentrifugation showed the protein in 50 mM Tris-HCl, pH 7.5, at 10 °C to be monodisperse with the expected molecular weight. Protein concentrations of the wild-type FNR were determined spectroscopically with an extinction coefficient of 10,000 M^{-1} cm^{-1} at 460 nm. The concentration of Y95A-FNR was determined by protein assay (DC protein assay kit; Bio-Rad) with wild-type FNR as a standard, and its extinction coefficient at 280 nm was calculated to be 47,800 M^{-1} cm^{-1}.

Apo-FNR was prepared by treatment with $CaCl_2$ (17). Wild-type FNR (100 μM) was diluted in 10 volumes of 100 mM Tris-HCl (pH 8.5) containing 3 M $CaCl_2$, 1 mM dithiothreitol, 0.1 mM EDTA, 17% glycerol (v/v), and 100 mM Gdm-HCl. After incubation at 4 °C for 2 h, the solution was passed through a PD-10 column (Amersham Biosciences) pre-equilibrated with 100 mM Tris-HCl (pH 8.5), 1 mM dithiothreitol, 0.1 mM EDTA, 17% glycerol (v/v), and 100 mM Gdm-HCl. The amount of apo-FNR was estimated to be >99%, based on the absorption spectrum of the FAD moiety.

The enzymatic activity of FNR was analyzed by NADPH-cytochrome *c* reduction as described previously (20).

CD and Fluorescence Measurements—CD measurements were carried out in a J-720WI spectropolarimeter (Jasco). Cuvettes with pathlengths of 1 mm and 1 cm were used for far-UV and near-UV CD, respectively. The results are expressed as the mean residue ellipticity, $[\theta]$, defined as $[\theta] = 100\ \theta_{obs}/l\ c$, where θ_{obs} is the observed ellipticity in degrees, c is the molar concentration of residue, and l is the length of the light path in centimeters. The temperature was controlled at 10 °C with a Jasco PTC-348WI peltier system. The protein concentrations were 4 and 8 μM for far-UV and near-UV CD, respectively. The secondary structure contents were estimated from far-UV CD spectra using two programs, k2d (21) and Selcon (22).

Fluorescence emission spectra were recorded at 10 °C in 50 mM Tris-HCl, pH 7.5, using a F-4500 fluorometer (Hitachi). The excitation wavelength was 453 nm for the fluorescence spectrum of FAD. The protein concentration was 4 μM, and the temperature was kept at 10 °C in a thermostatically controlled water bath.

SAXS Measurements—SAXS measurements were performed at the BL-10C small angle installation of the Photon Factory at the National Laboratory for High Energy Physics (Tsukuba, Japan). The sample solution in a cell with a pathlength of 1 mm was irradiated with a monochromatic x-ray beam (1.5 Å). The measurements were carried out at 10 °C with a thermostatically controlled cell holder. The protein concentrations were 50–400 μM. X-ray scattering intensities in the small angle region are given as $I(Q) = I(0)\ \exp(-\ R_g^2\ Q^2/3)$, where Q and $I(0)$ are momentum transfer and intensity at 0 scattering angle. Q is defined by $Q = (4\ \pi \sin \theta)/\lambda$, where 2θ and λ are the scattering angle and the wavelength of the x-rays, respectively. The radius of gyration (R_g) value was obtained from the slope of the Guinier plot. Data analysis was performed using the IGOR Pro data analysis program (WaveMetrics, Inc.). The $P(r)$ functions were evaluated using the GNOM program (23).

Gdm-HCl Denaturation—Equilibrium denaturation experiments with Gdm-HCl were performed at 10 °C. The protein solutions in various concentrations of Gdm-HCl were preincubated for at least 4 h at 10 °C before the experiments. The transitions were followed by far-UV CD and fluorescence of FAD. For CD measurements, the changes in ellipticity at 222 nm were recorded. The relative fluorescence intensities were recorded at 530 nm with an excitation wavelength of 453 nm. The resulting transition curves were analyzed by nonlinear least squares curve fitting, assuming a two-state transition (24) as shown in the following equation.

$$[\text{Signal}] = \{(a + b[\text{D}]) + (c + d[\text{D}])^*\exp[m([\text{D}] - C_M)/RT]\}/\{1 + \exp[m([\text{D}] - C_M)/RT]\} \quad \text{(Eq. 1)}$$

In this equation, [Signal] is either the ellipticity at 222 nm or fluorescence at 530 nm, a and c are the intercepts, and b and d are the slopes of the base lines for native and unfolded species, respectively, R is the gas constant, and T is a temperature. [D] and C_M are the concentration of Gdm-HCl for each experiment and the concentration at the midpoint of the reaction, respectively. ΔG_0, which is the free energy of unfolding in water, was calculated by the equation $\Delta G_0 = m\ C_M$, where m is the measure of cooperativity for the transition.

Affinity Chromatography—The affinities of FNR and its derivatives to NADP$^+$ were measured using a HiTrap Blue prepacked column (Amersham Biosciences) containing 7 μM Cibacron 3G-A resin (5 ml), which is an NADP$^+$ analogue. The column was equilibrated with 50 mM Tris-HCl buffer (pH 7.5) using the Äkta Prime system (Amersham Biosciences) at 4 °C. FNR solutions in different conformational states at neutral pH were loaded onto the column and eluted with a linear

gradient of 0–2 M NaCl in the same buffer at a flow rate of 2 ml min^{-1}. Elution of FNR was monitored by the absorption at 280 nm. For chromatography in the presence of $NADP^+$, 0.5 mM $NADP^+$ was present in the buffers and protein samples. Elution was detected by protein assay because of the overlapping absorption of protein and $NADP^+$.

FAD Titration—FNR holoenzyme is practically nonfluorescent, whereas FNR molecules unbound to FNR show intense fluorescence at around 530 nm. The reconstitution of holoenzyme from apo-FNR was detected by FAD titration assay (17). The excitation wavelength was 453 nm, and a cuvette with a pathlength of 5 mm was used. Protein concentrations were 0.3–1.0 μM in 50 mM Tris-HCl at pH 7.5. The protein solutions containing various amounts of FAD were incubated for 3 days at 4 °C before fluorescence measurements.

RESULTS

Conformational Properties of Holo-FNR at Various pH Values—We first characterized the acid-induced structural changes in holo-FNR and its relationship with FAD binding ability using CD and fluorescence spectroscopy. Consistent with the results of x-ray crystallography, the far-UV CD spectrum of holo-FNR in its native state at pH 6.0 exhibited a shape typical of α/β proteins (Fig. 2*A*). At pH 2.4, holo-FNR showed disruption of its secondary structures to some extent but retained a substantial amount of secondary structure. This suggested the accumulation of partially folded species at pH 2.4.

Holo-FNR contains its cofactor, FAD, at the interface between the FAD and $NADP^+$ binding domains. FAD in its free form at neutral pH shows intense fluorescence around 460–700 nm when excited at 453 nm. In contrast, the fluorescence is quenched upon binding to FNR polypeptide (25). At pH 2.4, the fluorescence of FAD increased, showing that the cofactor was released upon denaturation of FNR (Fig. 2*B*). The pH titration curve obtained by fluorescence analysis coincided well with the transition obtained by far-UV CD (Fig. 2*C*). This indicated that pH-dependent dissociation of FAD is a process coupled with the acid unfolding of FNR.

Gdm-HCl Denaturation—The equilibrium unfolding transitions induced by Gdm-HCl were followed by far-UV CD and fluorescence of FAD at pH 2.4 or pH 6.0, 10 °C (Fig. 3). For holo-FNR, a cooperative unfolding transition was obtained by far-UV CD. The transition curve was consistent with the dissociation of FAD monitored by the fluorescence of FAD (Fig. 3; Table I). These observations suggested that the denaturation transition by Gdm-HCl is well approximated by a cooperative two-state mechanism from the native to unfolded state coupled with the loss of FAD binding ability.

The conformation of the acid-induced unfolded state at pH 2.4 was more structured than that of Gdm-HCl unfolding (Figs. 2 and 3). Interestingly, a moderately cooperative unfolding transition of the acid-denatured state was induced by Gdm-HCl at pH 2.4. This further supported the idea that persistent structures remained to some extent at pH 2.4 in the absence of denaturants (Fig. 3). However, the loss of cooperativity for the unfolding transition at pH 2.4 relative to the transition at pH 6.0 was well represented by parameter *m,* obtained by curve-fitting analysis on the basis of a two-state mechanism (Table I). The *m* value is considered to be correlated with changes in the accessible surface area upon unfolding.

Structural Properties of FAD-depleted FNR at Neutral pH—Fig. 4*A* shows the far-UV CD spectra of various species of FNR at pH 7.5 and 10 °C. By removal of FAD, apo-FNR showed smaller amplitudes of negative ellipticity at 200–235 nm than the holo-protein. Interestingly, the Y95A mutant showed a far-UV CD spectrum similar to that of apo-FNR, indicating that Y95A-FNR assumes a conformation similar to that of apo-FNR.

The near-UV CD spectrum of holo-FNR showed a sharp positive peak and negative peaks at 275 and 295 nm, respectively (Fig. 4*B*). Movements of particular residues among 32 aromatic amino acids in maize FNR (12 phenylalanines, 6 tryptophans,

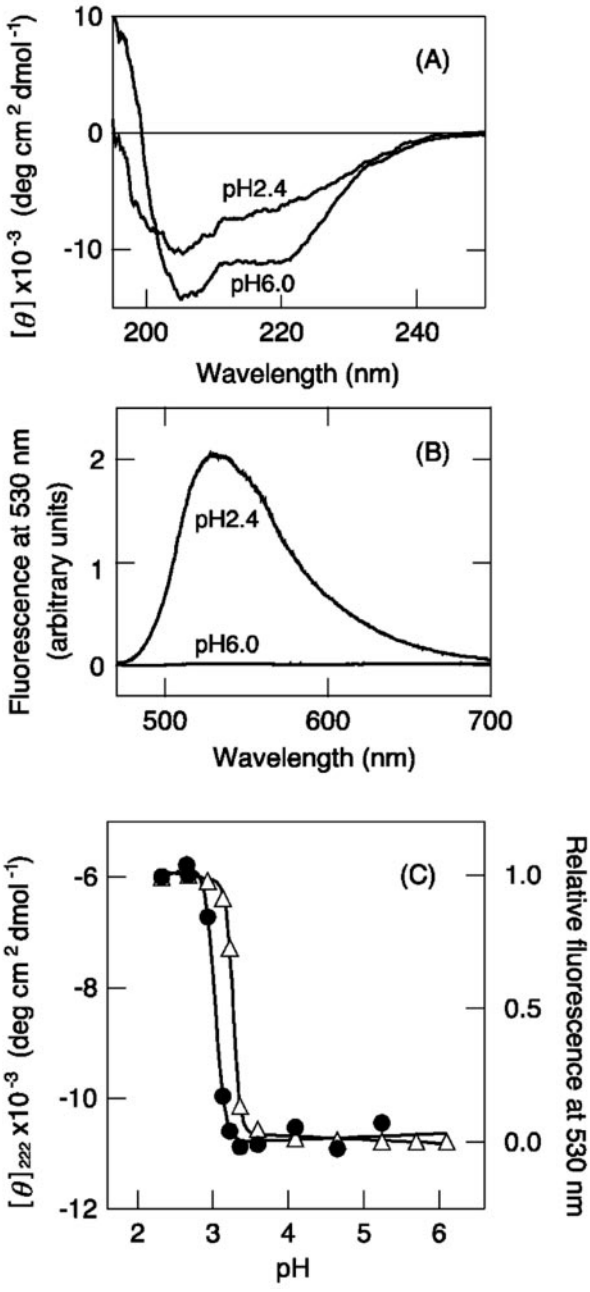

FIG. 2. **pH-dependent structural changes of FNR.** *A*, CD spectra of holo-FNR at pH 6.0 and pH 2.4. *B*, fluorescence spectra of holo-FNR at pH 6.0 and pH 2.4. *C*, pH titration of holo-FNR monitored by ellipticity at 222 nm (●) and fluorescence intensity at 530 nm (△). The buffers used were 50 mM glycine-HCl (pH 2.3–3.0), 50 mM citrate-NaOH (pH 3.1–5.7), and 50 mM phosphate-NaOH (pH 5.8–6.3), at 10 °C.

and 14 tyrosines) are restricted within the tertiary structure of holo-FNR. Y95A-FNR showed a spectrum similar to that of holoprotein but with lower amplitude at 260–320 nm. This suggested that the tertiary structure was disrupted to some extent in Y95A-FNR or that the intrinsic contribution of tyrosine 95 to this CD spectrum was relatively large. On the other hand, apo-FNR exhibited no clear peak at around 275 nm and a small but distinctive negative peak at 295 nm.

The broad Cotton effects of holo-FNR in the CD region around 400 nm were probably due to the bound FAD, considering the observation that apo- and Y95A-FNR with no bound FAD indicated no such peaks.

SAXS Data—Fig. 5*A* shows Guinier plots (ln (*I*(*Q*)) *versus* Q^2) for various species of FNR. The slope of the plot in the low

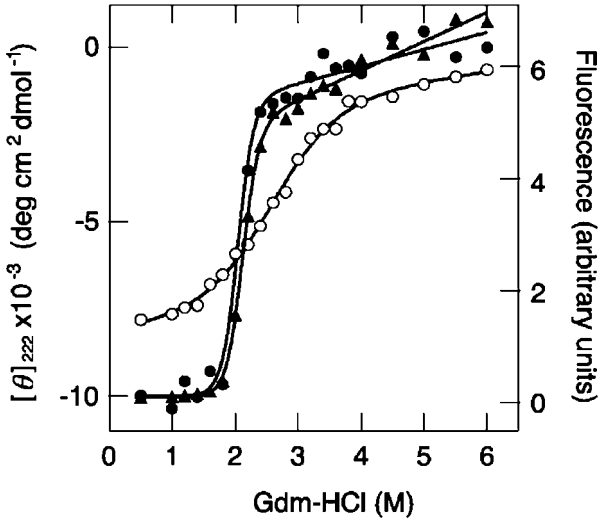

FIG. 3. **Gdm-HCl-induced denaturation of holo-FNR monitored by ellipticity at 222 nm and fluorescence intensity at 530 nm with an excitation wavelength of 453 nm.** ●, ellipticity at pH 6.0; ▲, fluorescence emission of FAD at pH 6.0; ○, ellipticity at pH 2.4. The *lines* correspond to the results of curve fitting.

TABLE I
Thermodynamic parameters for the unfolding of holo-FNR in Gdm-HCl at 10 °C

pH	ΔG_0[a]	m[b]	C_M[c]	Method
	(kcal mol^{-1})	*(kcal mol^{-1} M^{-1})*	*(M)*	
6.0	−9.15 ± 1.91	4.48 ± 0.91	2.04	Ellipticity at 222 nm
6.0	−9.18 ± 1.06	4.34 ± 0.49	2.11	Fluorescence at 530 nm[d]
2.4	−2.79 ± 0.66	1.08 ± 0.21	2.58	Ellipticity at 222 nm

[a] Free energy difference between the native and unfolded states in water.
[b] The cooperativity index of the transition.
[c] The midpoint Gdm-HCl concentration of denaturation.
[d] Fluorescence emission at 530 nm with an excitation wavelength of 453 nm.

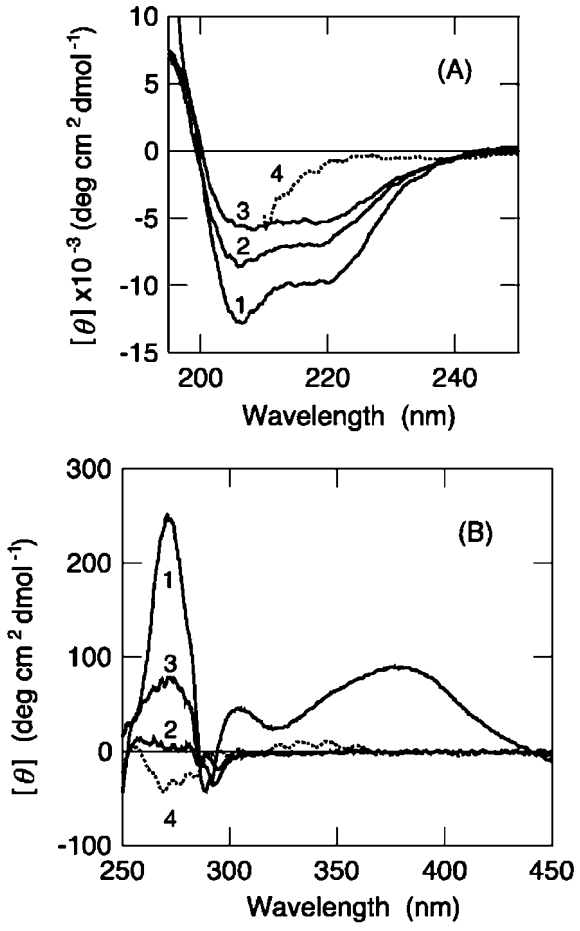

FIG. 4. **CD spectra at (*A*) far- and (*B*) near-UV and visible regions for various conformational states of FNR in 50 mM Tris-HCl, pH 7.5, at 10 °C.** Holo-FNR (*1*), apo-FNR (*2*), Y95A-FNR (*3*), and unfolded state (*4*) in 4.0 M Gdm-HCl (*dotted lines*).

Q region, *i.e.* small angle, gives the most reliable estimate of radius of gyration (R_g), informative for the size and compactness of polypeptide chains (26). Because the R_g value is dependent on protein concentration, the corrected R_g values of FNR in the different conformational states shown above were obtained by extrapolating to zero protein concentration. The R_g value for holo-FNR was estimated to be 27.0 Å (Table II), whereas apo-FNR had a larger R_g value of 48.7 Å. This value was surprisingly consistent with the R_g of Y95A-FNR (48.6 Å), another FAD-depleted form. However, these values for FAD-depleted FNR were smaller than the R_g of unfolded protein in 4.0 M Gdm-HCl (63.1 Å). Consistent with the results obtained by CD spectroscopy, these experimental results supported the idea that apo- and Y95A-FNR assume similar partially folded conformations.

The Kratky plot, $I(Q) \times Q^2$ *versus* Q, for holo-FNR had a sharp peak at $Q = 0.07$ (Å^{-1}) and a pattern typical of the native state of a globular protein (Fig. 5*B*). In contrast, that in the presence of 4.0 M Gdm-HCl was typical of a highly denatured random coil structure, *i.e.* a plateau in the low Q region followed by a monotonic increase in $I(Q) \times Q^2$ at higher Q values. The plots for apo- and Y95A-FNR showed intermediate characteristics. They were moderately disordered relative to holo-FNR but still possessed globular components represented by broad peaks around $Q = 0.06$ (Å^{-1}). The small shifts of such peaks for apo- and Y95A-FNR relative to those of holo-FNR suggested more expanded conformations for apo- and Y95A-FNR. The information regarding molecular shape for each conformational species is summarized in Table II.

Information on shape and size can also be obtained from the distribution function, $P(r)$. Fig. 5*C* shows the $P(r)$ functions for holo- and Y95A-FNR. The $P(r)$ function for holo-FNR had a single peak at 26 Å and the maximum chord of the molecule, d_{max}, was 93 Å. The slight distribution over 60 Å could be due to the influence of the fluctuating N-terminal flared tail (Fig. 1*A*). On the other hand, $P(r)$ of Y95A-FNR had a single peak at 37 Å, and d_{max} was 121 Å. These distances were clearly larger than the corresponding values of holo-FNR, consistent with the results obtained by analysis of Guinier plots. Unlike the $P(r)$ expected for the complete spherical globule, the $P(r)$ function for this mutant had a broad distribution at a higher r value but no distinctive shoulder. The curve could be expressed as a biphasic function as shown for the molten globule intermediate of apomyoglobin (27).

Affinity Chromatography—The native holo-FNR consists of two distinctive folding units, *i.e.* the FAD and NADP$^+$ binding domains. Therefore, it is possible that the partially folded species of FNR formed by the removal of FAD contains a native-like well-defined structure in at least one of the two domains.

Indeed, Y95A mutant protein showed significantly high affinity to Cibacron Blue resin with an NADP$^+$ analogue (Fig. 6). The elution time for Y95A-FNR was similar to that for holo-FNR. These observations suggested that Y95A-FNR, which lacks a FAD molecule, might contain the persistent native-like folded NADP$^+$ binding domain. High affinity to this column was also observed for apo-FNR. Elution was shifted to a higher salt concentration than that for holo-FNR. This was probably due to the smaller amount of protein applied to reduce the

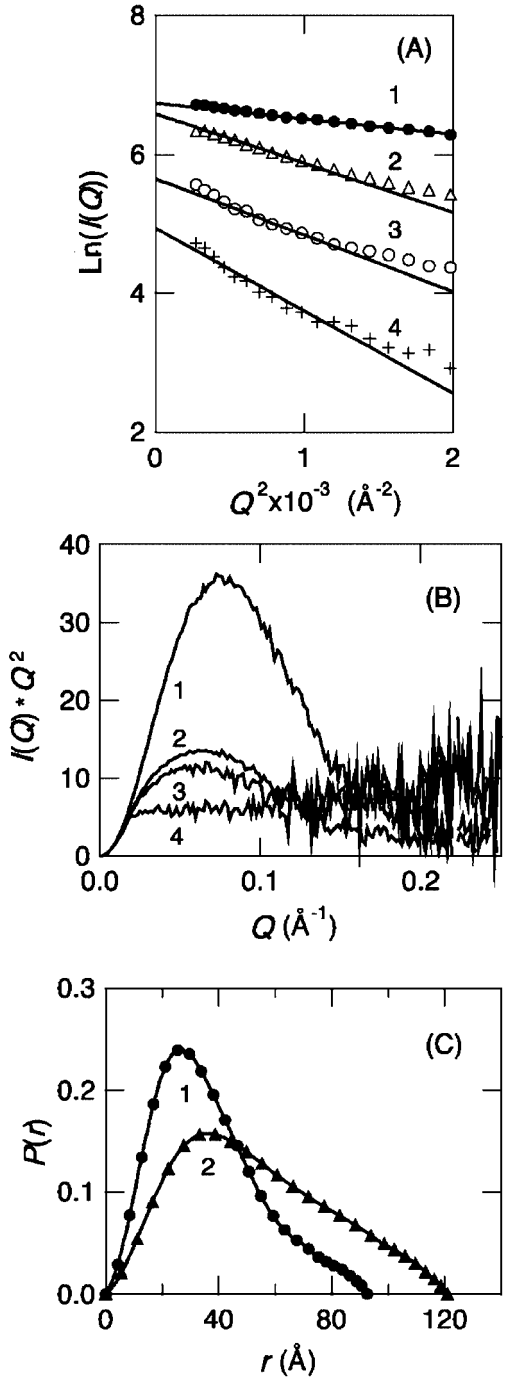

FIG. 5. **Guinier plots (*A*), Kratky plots (*B*), and *P*(*r*) functions (*C*) of various conformational states of FNR by SAXS at 10 °C.** Holo-FNR (*1*), Y95A-FNR (*2*), apo-FNR (*3*), and unfolded state (*4*) in 4.0 M Gdm-HCl. In *A*, *symbols* indicate raw data, and *lines* are the results of curve-fitting analysis. Each plot is shifted along the ln *I*(*Q*) axis for clarity.

possibility of forming a precipitate: apo-FNR was prone to aggregate at high protein concentrations. As a negative control, ovalbumin was eluted in the flow-through fraction. Moreover, to confirm the specificity of the interaction of apo-FNR with the $NADP^+$-bound resin, the effects of $NADP^+$ in the buffer were examined. Both holo- and apo-FNR (particularly apo-FNR) eluted faster with the addition of 0.5 mM $NADP^+$ to the sample and elution buffers than they did in its absence. These results showed that $NADP^+$ in solvent competes with $NADP^+$ on the resin, although the competition at 0.5 mM $NADP^+$ was not perfect and did not completely prevent binding to the resin.

Reconstitution and Reversibility—The reconstitution of holo-FNR from apo- and Y95A-FNR was attempted by adding FAD to these FNR derivatives at neutral pH. The equilibrium binding curve of FAD to apo-FNR was followed by quenching of the added FAD fluorescence upon binding to FNR (Fig. 7). The fluorescence was completely quenched when a small amount of FAD (<60% of FNR molecule) was added to the solution, suggesting specific binding of FAD to FNR molecules. However, additional quenching was no longer observed in the presence of FAD at >60% of FNR molecules.

The recovery yield of holo-FNR was also estimated by monitoring the enzymatic activity. The reconstitution yield estimated by enzymatic activity (57%) was consistent with the incorporation of FAD (60%) estimated by fluorescence quenching. In contrast to apo-FNR, Y95A-FNR did not show any quenching of FAD fluorescence as well as the enzymatic activity. This was expected because Y95A-FNR probably lacks the ability to bind the FAD molecule due to the removal of the stacking interaction of Tyr^{95} side chain to the isoalloxazine ring of FAD.

DISCUSSION

Structure and Stability of the Intermediates—The present study showed that two apoenzymes of FNR produced by different methods assume partially folded structures rather than being fully unfolded (Tables I and II). The reconstitution of holo-FNR was demonstrated by adding FAD to apo-FNR, suggesting that the partially folded species is a productive intermediate rather than a misfolded state. Residual tertiary structures are present to some extent in apo-FNR, as evident from the peaks in the near-UV CD spectrum (Fig. 4*B*). SAXS analysis demonstrated that the apo state retains a globular component, although it is more expanded compared with the native state of holo-FNR (Fig. 5). Interestingly, the ability of FAD-depleted FNR species to bind to $NADP^+$ suggested that some native-like structure is retained at least around the binding site in the $NADP^+$ binding domain (Fig. 6). On the other hand, Y95A-FNR had no affinity to a ferredoxin-immobilized Sepharose column (data not shown). These partially folded states of apoenzymes have spectroscopic features similar to the structure formed at pH 2.4 for holo-FNR as well as Y95A mutant at neutral pH (Figs. 2 and 4, Table II). The molten globule intermediates of other proteins are also known to be stabilized at acidic pH and particularly in the presence of added anions (28, 29). The moderately cooperative transition determined by the CD spectra of acid-unfolded FNR confirmed the presence of residual secondary structure (Fig. 3).

Partially folded intermediates of multidomain proteins can be composed of well-structured and unstructured domains. For instance, the folding intermediate of hen lysozyme has a well-defined α-domain and a fluctuating β-domain (30). Importantly, experiments on single-domain proteins have suggested that they can also be decomposed into small folding units, *i.e.* subdomains (31, 32). This implies that even a partially folded state of a single-domain protein, which corresponds to the classical molten globule, can contain folded and unfolded subdomains (33). The molten globule was originally defined as an intermediate conformation with a substantial amount of native-like secondary structure but fluctuating tertiary contacts (34, 35). However, experiments on partially folded states of proteins have indicated that there are a variety of intermediate states in terms of the contribution of specific tertiary contacts to stability. In addition, the criteria of a "molten globule" have recently been extended so as to be more realistic in describing a partially folded state. In this sense, the structural properties of apo- and Y95A-FNR can be considered as variations of the molten globule state.

One of the most important results obtained here was the

TABLE II
Structural parameters of various states of maize FNR

Conditions	α-Helix[a]	β-Sheet	Reminder	$[\theta]_{222}$	$[\theta]_{270}$	R_g	Activity[b]	Shape[c]	$NADP^+$ affinity[d]
	%	%	%	*deg cm² mol⁻¹*	*deg cm² mol⁻¹*	*Å*	%		
holo-FNR, pH 7.5	27/26 (26)[e]	18/39 (24)	55/35 (50)	−9300	248	27.0 ± 0.3	100	Highly globular	+
apo-FNR, pH 7.5	17/19	30/53	53/30	−6000	2	48.7 ± 1.2	0.1	Globular	+
Y95A-FNR, pH 7.5	16/12	31/59	53/29	−4800	71	48.6 ± 0.5	0.2	Globular	+
unfolded FNR, pH 2.4	15/21	29/48	55/30	−5900	−37	49.1 ± 1.2	ND[f]	Globular	ND
unfolded FNR, Gdm-HCl[g]	5/6	47/60	48/33	−760	−45	63.1 ± 2.1	0	Chain-like	ND

[a] The secondary structure contents estimated from far-UV CD spectra calculated by k2d/Selcon.
[b] Cytochrome *c* reductase activity.
[c] Molecular shape estimated from the shapes of Kratky plots.
[d] Determined by the elution from Cibacron Blue affinity chromatography.
[e] FNR x-ray structure.
[f] ND, not determined.
[g] The unfolded protein was obtained in 4.0 M Gdm-HCl, pH 7.5, 10 °C.

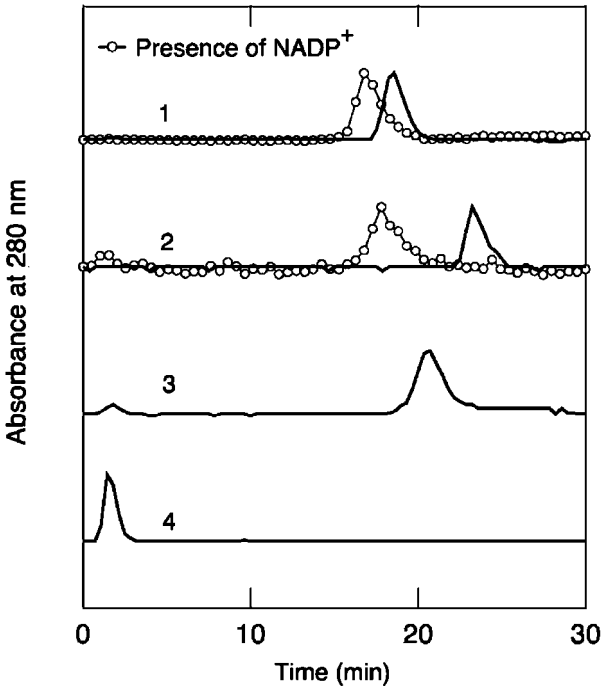

FIG. 6. **Cibacron Blue affinity chromatography of various FNR species.** $NADP^+$-binding protein-sensitive affinity chromatography of various conformational states of FNR. *1,* holo-FNR; *2,* apo-FNR; *3,* Y95A-FNR; *4,* ovalbumin. ○, the presence of 0.5 mM $NADP^+$. Proteins were eluted with a linear gradient of 0–2 M NaCl between 10 and 20 min.

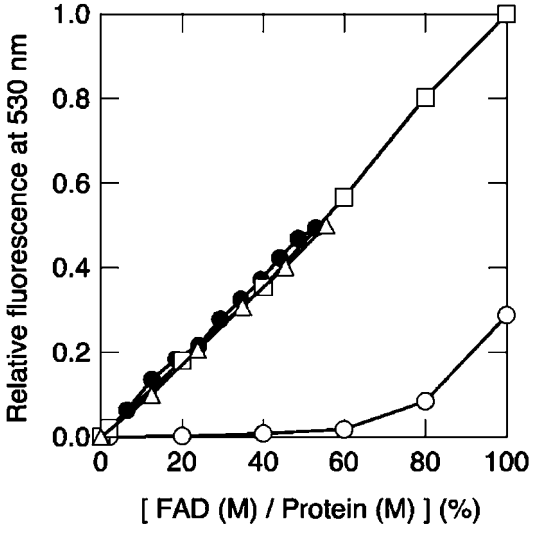

FIG. 7. **FAD titration of various conformational states of FNR monitored by fluorescence of FAD measured at pH 7.5, 10 °C.** ●, holo-FNR; ○, apo-FNR; △, Y95A-FNR; □, buffer in the absence of protein.

persistence of the $NADP^+$ binding domain in the partially folded FNR species. The far-UV CD spectrum of apo-FNR did not change effectively in the presence or absence of $NADP^+$ (data not shown). This means that $NADP^+$ does not induce further conformational rearrangement of the $NADP^+$ binding domain, consistent with the persistence of the $NADP^+$ binding domain. The far-UV CD spectra of these proteins showed ~50% of the intensity of holo-FNR. We estimated the secondary structure contents of various forms of FNR on the basis of far-UV CD spectra (Table II). The secondary structure contents for holo-FNR were consistent with those determined from x-ray crystallographic data (*i.e.* 26% α-helix and 24% β-sheet). For the FAD-depleted species, α-helix content decreased, whereas β-sheet content did not decrease notably. Disordering of the α-helix in the FAD binding domain probably explains the decrease of α-helix content. However, because the estimation of β-sheet content from CD is often unreliable, the apparent increases in amount of β-sheet observed for various non-native species cannot be discussed further.

The present results did not specify whether apo- and Y95A-FNR have either the partially folded conformation or an expanded structure with respect to the FAD binding domain. Nevertheless, comparison of R_g values of several conformational states of FNR and other proteins suggested that the FAD binding domain may be relatively expanded rather than assuming a compact structure. SAXS results of several proteins showed that the R_g values of partially folded intermediates are 10–30% larger than the values of the native structures (36). On the other hand, the R_g value of FAD-depleted FNR was 81.5% larger than the value of holo-FNR. It is likely that the FAD binding domain assumes a rather expanded conformation in FAD-depleted FNR.

Implication for Folding of Multidomain Proteins—For proteins consisting of several domains, the stability and cooperativity of the isolated single domains can be lower than those in the completely folded protein, in which they are supported by the neighboring domains (37, 38). The agreement of Gdm-HCl or acid unfolding transitions of holo-FNR with the release of FAD (Fig. 3) suggested that the process can be approximated by the two-state transition. This can be explained by the location of the FAD molecule at the interface between the FAD and $NADP^+$ binding domains of FNR. Such interactions can substantially increase the cooperativity of unfolding transition by stabilizing both domains in the native state. Consistent with this, the structural properties of FAD-depleted FNR suggested

that this cooperativity is lost by removal of the cofactor located at the interface of the two domains.

An intermediate structure similar to apo-FNR at neutral pH has also been stabilized under unfolding conditions at pH 2.4. In the electrostatic surface potential map of the native structure of holo-FNR, it is obvious that the FAD binding domain has a positively charged surface, whereas the $NADP^+$ binding domain has negative electrostatic potential (Fig. 1*B*). This difference in the distribution of electric potential implies that the denaturation of the FAD binding domain can occur more readily at acidic pH than unfolding of the $NADP^+$ binding domain because of the preferential increase of positive charges and hence the electrostatic repulsion in the FAD binding domain. This could result in the formation of an acidic intermediate conformation similar to apo- and Y95A-FNR at neutral pH. The critical role of charge repulsion in protein stability has been indicated in several cases. For example, whereas aspergillopepsin II, an aspartic proteinase composed of many (20% of total) negatively charged residues, is stable at acidic pH, it unfolds at alkaline pH because of the negative charge repulsion (39).

Comparison with Other Proteins with Cofactors—The results presented here suggested the accumulation of partially folded FNR upon removal of the cofactor, FAD. Many proteins show a less structured conformation relative to the native state upon release of a cofactor at neutral pH. One of the most extreme cases of this is horse cytochrome *c* (40). This protein has a covalently bound heme group, and removal of this prosthetic group by treatment with Ag_2SO_4 produces an apoprotein that assumes a relatively unstructured compact state at neutral pH. On the other hand, apomyoglobin derived from removal of a bound heme group in holomyoglobin retains a folded structure with 55% α-helical content (41, 42). In this respect, apo-FNR is more similar to apomyoglobin than to apocytochrome *c*. In contrast, flavodoxin is one of the most well-studied flavoproteins with regard to its stability and folding reaction (43, 44). The three-dimensional structure of this protein consists of only one domain with a binding site for a flavin mononucleotide, FMN, and assumes the native structure even after the removal of FMN.

Several lines of evidence suggest that multidomain flavoproteins including FNR have evolved by the assembly of some single-domain proteins, especially $NADP^+$-binding protein (13, 45). FNR may have evolved by such a mechanism. The ancestor of FNR might have had the ability to assume the native structure even without its cofactor at the early stage of evolution. For those proteins with cofactors, the relationship between protein evolution and stability related to cofactor binding is an exciting area of study that may reveal how the proteins have evolved.

Acknowledgments—We thank Dr. G. Kurisu for providing the atomic coordinates of maize leaf FNR prior to publication. The x-ray scattering measurements were performed with permission from the Program Advisory Committee of the Photon Factory (Proposal No. 99G354). We thank Dr. H. Kamikubo for helpful discussion on the analysis of SAXS data and H. Kato for assistance with measurements.

REFERENCES

1. Fink, A. L. (1995) *Annu. Rev. Biophys. Biomol. Struct.* **24,** 495–522
2. Arai, M., and Kuwajima, K. (2000) *Adv. Protein Chem.* **53,** 209–282
3. Jackson, S. (1998) *Folding Des.* **3,** R81–R91
4. Ferguson, N., Capaldi, A. P., James, R., Kleanthous, C., and Radford, S. E. (1999) *J. Mol. Biol.* **286,** 1597–1608
5. Fersht, A. R. (2000) *Structure and Mechanism in Protein Science*, pp. 543–553, Freeman, New York
6. Roder, H., and Colon, W. (1997) *Curr. Opin. Struct. Biol.* **7,** 15–28
7. Chamberlain, A. K., Handel, T. M., and Marqusee, S. (1996) *Nat. Struct. Biol.* **3,** 782–787
8. Zitzewitz, J. A., and Matthews, C. R. (1999) *Biochemistry* **38,** 10205–10214
9. Fischer, K. F., and Marqusee, S. (2000) *J. Mol. Biol.* **302,** 701–712
10. Peng, Z. U., and Wu, L. C. (2000) *Adv. Protein Chem.* **53,** 1–30
11. Hopfner, K. P., Kopetzki, E., Kresse, G. B., Bode, W., Huber, R., and Engh, R. A. (1998) *Proc. Natl. Acad. Sci. U. S. A.* **95,** 9813–9818
12. Lang, D., Thoma, R., Henn-Sax, M., Sterner, R., and Wilmanns, M. (2000) *Science* **289,** 1546–1550
13. Vallon, O. (2000) *Proteins Struct. Funct. Genet.* **38,** 95–114
14. Baker, D. (2000) *Nature* **405,** 39–42
15. Arakaki, A. K., Ceccarelli, E. A., and Carrillo, N. (1997) *FASEB J.* **11,** 133–140
16. Kurisu, G., Kusunoki, M., Katoh, E., Yamazaki, T., Teshima, K., Onda, Y., Kimita-Ariga, Y., and Hase, T. (2001) *Nat. Struct. Biol.* **8,** 117–121
17. Zanetti, G., Cidaria, D., and Curti, B. (1982) *Eur. J. Biochem.* **126,** 453–458
18. Onda, Y., Matsumura, T., Kimita-Ariga, Y., Sakakibara, H., Sugiyama, T., and Hase, T. (2000) *Plant Physiol.* **123,** 1037–1045
19. Matsumura, T., Sakakibara, H., Nakano, R., Kimata, Y., Sugiyama, T., and Hase, T. (1997) *Plant. Physiol.* **114,** 653–660
20. Hase, T., Mizutani, S., and Mukohata, Y. (1991) *Plant Physiol.* **97,** 139–1401
21. Andrade, M. A., Chacon, P., Merelo J. J., and Moran, F. (1993) *Protein Eng.* **6,** 383–390
22. Sreerama, N., and Woody, R. W. (1994) *Biochemistry* **33,** 10022–10025
23. Svergun, D. I., Semenyuk, A. V., and Feigin, L. A. (1988) *Acta Crystallogr. Sect. A* **44,** 244–250
24. Pace, C. N. (1986) *Methods Enzymol.* **131,** 266–280
25. Forti, G. (1966) *Brookhaven Symp. Biol.* **19,** 195–201
26. Glatter, O., and Kratky, O. (1982) *Small-angle X-ray Scattering*, Academic Press, New York
27. Kataoka, M., Nishi, I., Fujisawa, T., Ueki, T., Tokunaga, F., and Goto, Y. (1995) *J. Mol. Biol.* **249,** 215–228
28. Goto, Y., Calciano, L. J., and Fink, A. L. (1990) *Proc. Natl. Acad. Sci. U. S. A.* **87,** 573–577
29. Goto, Y., Takahashi, N., and Fink, A. L. (1990) *Biochemistry* **29,** 3480–3488
30. Radford, S. E., Dobson, C. M., and Evans, P. A. (1992) *Nature* **358,** 302–307
31. Fersht, A. R. (1995) *Proc. Natl. Acad. Sci. U. S. A.* **92,** 10869–10873
32. Philipp, S., Kim, Y. M., Durr, I., Wenzl, G., Vogt, M., and Flecker, P. (1998) *Eur. J. Biochem.* **251,** 854–862
33. Privalov, P. L. (1996) *J. Mol. Biol.* **258,** 707–725
34. Ohgushi, M., and Wada, A. (1983) *FEBS Lett.* **164,** 21–24
35. Dobson, C. M. (1994) *Curr. Biol.* **4,** 636–640
36. Kataoka, M., and Goto, Y. (1996) *Folding Des.* **1,** R107–R114
37. Mayr, E.-M., Jaenicke, R., and Glockshuber, R. (1997) *J. Mol. Biol.* **269,** 260–269
38. Jaenicke, R., and Böhm, G. (1998) *Curr. Opin. Struct. Biol.* **8,** 738–748
39. Kojima, M., Tanokura, M., Maeda, M., Kimura, K., Amemiya, Y., Kihara, H., and Takahashi, K. (2000) *Biochemistry* **39,** 1364–1372
40. Hamada, D., Hoshino, M., Kataoka, M., Fink, A. L., and Goto, Y. (1993) *Biochemistry* **32,** 10351–10358
41. Hughson, F. M., Wright, P. E., and Baldwin, R. L. (1990) *Science* **249,** 1544–1548
42. Eliezer, D., Yao, J., Dyson, H. J., and Wright, P. E. (1998) *Nat. Struct. Biol.* **5,** 148–155
43. Genzor, C. G., Beldarrain, A., Gomez-Moreno, C., Lopez-Lacomba, J. L., Cortijo, M., and Sancho, J. (1996) *Protein Sci.* **7,** 1376–1388
44. Steensma, E., and van Mierlo, C. P. M. (1998) *J. Mol. Biol.* **282,** 653–666
45. Porter, T. D., and Kasper, C. B. (1986) *Biochemistry* **25,** 1682–1687
46. Koradi, R., Billeter, M., and Wüthrich, K. (1996) *J. Mol. Graphics* **14,** 51–55

Partially Folded Structure of Flavin Adenine Dinucleotide-depleted Ferredoxin-NADP $^{+}$ Reductase with Residual NADP^{+} Binding Domain

Masahiro Maeda, Daizo Hamada, Masaru Hoshino, Yayoi Onda, Toshiharu Hase and Yuji Goto

J. Biol. Chem. 2002, 277:17101-17107.
doi: 10.1074/jbc.M112002200 originally published online February 28, 2002
